Magnetic nanoparticles for enhancing the effectiveness of ultrasonic hyperthermia

A. Józefczak,[1,a)] K. Kaczmarek,[1] T. Hornowski,[1] M. Kubovčíková,[2] Z. Rozynek,[1] M. Timko,[2] and A. Skumiel[1]
[1]*Institute of Acoustics, Faculty of Physics, Adam Mickiewicz University, Umultowska 85, 61-614 Poznań, Poland*
[2]*Institute of Experimental Physics, Slovak Academy of Sciences, Watsonova 47, 040 01 Košice, Slovakia*

(Received 25 April 2016; accepted 21 June 2016; published online 30 June 2016)

Ultrasonic hyperthermia is a method of cancer treatment in which tumors are exposed to an elevated cytotoxic temperature using ultrasound (US). In conventional ultrasonic hyperthermia, the ultrasound-induced heating in the tumor is achieved through the absorption of wave energy. However, to obtain appropriate temperature in reasonable time, high US intensities, which can have a negative impact on healthy tissues, are required. The effectiveness of US for medical purposes can be significantly improved by using the so-called sonosensitizers, which can enhance the thermal effect of US on the tissue by increasing US absorption. One possible candidate for such sonosensitizers is magnetic nanoparticles with mean sizes of 10–300 nm, which can be efficiently heated because of additional attenuation and scattering of US. Additionally, magnetic nanoparticles are able to produce heat in the alternating magnetic field (magnetic hyperthermia). The synergetic application of ultrasonic and magnetic hyperthermia can lead to a promising treatment modality. *Published by AIP Publishing*. [http://dx.doi.org/10.1063/1.4955130]

Hyperthermia is a type of cancer treatment in which the target tumor is exposed to elevated temperatures (41–46 °C).[1] Hyperthermia has been widely used as a medical procedure for cancer treatment because of its simple implementation, low cost, and reduced complication.[2] Different techniques have been used to generate thermal energy, including ultrasound (US). At ultrasound intensities lower than either thermal ablation or tissue disintegration, slight temperature elevations are achieved and the treatment is classified as hyperthermia.[3] Ultrasound has considerable physical advantages over most techniques since the beam can be focused strongly because of its short wavelength.[4] In conventional ultrasonic hyperthermia, the ultrasound-induced heating is achieved by the attenuation of ultrasonic wave in the tissue and conversion of its energy into heat. This process involves both scattering and absorption, although it is dominated by the latter, and indeed, the scattered wave is subsequently absorbed.[3] The therapeutic effect of ultrasound irradiation can also be achieved through the physical destruction of cellular structures because of cavitation processes.[5] However, to obtain appropriate temperatures in reasonable time, high ultrasound wave intensities (1–100 W/cm^2), which can have a negative impact on healthy tissues,[6] are required. The effectiveness of ultrasounds for sonodynamic therapy can be significantly improved by using the so-called sonosensitizers, which can enhance the thermal effect of ultrasound on the tissue by increasing US absorption. One possible candidate for such sonosensitizers is nanoparticles with mean sizes of 10–300 nm, which can be efficiently heated in aqueous suspensions because of additional attenuation and scattering of ultrasounds. Sviridov *et al.*[7] have shown that aqueous suspensions of porous silicon nanoparticles undergo significant heating compared with pure water under therapeutic ultrasonic (US) irradiation. Nanoparticle-induced heating can result in a significant increase of the mean temperature of aqueous suspensions, which is 1.5–2 times higher than that for pure water.[7] Other nanoparticles were also tested as candidates for sonosensitizers, e.g., gold or graphene oxide particles, which proved to exhibit good heating efficiency.[8] In this work, however, we focused on superparamagnetic iron oxide nanoparticles (SPIONs) coated with a biocompatible shell. SPIONs are a single domain and possess a magnetic moment proportional to the volume of the particle. Additionally, magnetic nanoparticles can have multifunctional characteristics with complimentary roles.[9] Magnetic nanoparticles by themselves are able to produce localized heating of the sample that can be fine-tuned and controlled by the alternating magnetic field (AMF).[10] The aforementioned types of particles, i.e., diamagnetic gold nanoparticles, nonmagnetic porous silicon, and graphene oxide nanoparticles, do not offer such possibility. In a non-homogeneous alternating magnetic field, magnetic nanoparticles oscillate mechanically and can also generate ultrasound waves,[11,12] which can be used for magnetoacoustic imaging of diseased tissues.[13] Also microbubbles coated with magnetic nanoparticles can have a wide range of biomedical applications. Under the influence of ultrasonic wave, such microbubbles start to vibrate and if the pressure is sufficient enough, some nanoparticles can free themselves and travel away from the bubble.[14]

In this work, Fe_3O_4 nanoparticles were prepared through the chemical coprecipitation using ferric and ferrous salts in alkali medium.[15] The nanoparticles were coated with the surfactant sodium oleate ($C_{17}H_{33}COONa$) to prevent the agglomeration of the particles. The magnetite particles stabilized by oleate bilayer were dispersed in water. Agglomerates were

a)Author to whom correspondence should be addressed. Electronic mail: aras@amu.edu.pl.

removed through centrifugation (9000 rpm for 30 min). Transmission electron microscopy (TEM) images of the prepared magnetite particle and their size histogram are presented in Fig. 1(a). Additionally, the magnetometry measurements (SQUID) were performed (Fig. 1(b)) to determine both the particle size distribution (inset in Fig. 1(b)) and the volume concentration of the magnetite particles in suspension, which is 70 mg/ml. The peak value of the particle size distribution obtained from the SQUID corresponds to that from the particle size distribution determined from the TEM image, and that is around 6 nm.

The hyperthermia experiments were performed in a tissue-mimicking phantom. Over the last decade, tissue mimicking phantoms have been routinely used as a powerful tool for the performance testing of ultrasonic hyperthermia. The gel form of agar has been widely used by researchers as a phantom of human tissue because its acoustic characteristic (sound speed near 1540 m/s, density near 1.0 g/cm^3, and attenuation coefficient near 0.5 dB/cm/MHz) is very similar to that of the human tissue.[16]

Two types of agar phantom samples were prepared for measurements: pure agar gel without any added scattering material and agar gel with magnetic nanoparticles. Agar powder was dissolved in hot distilled water. During the production process of the gel, the magnetic nanoparticle scatterers were added. Samples were made by varying the weight concentration of agar from 3% to 10% (w/v). The weight concentrations of Fe_3O_4 particles were 8 and 16 mg/ml.

The apparatus used for the ultrasonic hyperthermia experiments consists of a signal generator joined to a high-frequency power amplifier, which feeds the continuous wave signal into a broadband power amplifier that drives the ultrasonic Langevin transducer. The transducer consists of two piezoceramic rings mechanically pressed with the help of a steel bolt as well as back (steel) and front (aluminum) vibrating masses. The front acoustic mass vibrates with an aluminum concentrator, the length of which corresponds to half of the ultrasonic wave ($\lambda/2 \cong 125$ mm).[17] The tip of the concentrator is connected to the tissue-mimicking phantom. The emitter area was 2.5 cm^2. The investigation was performed for constant ultrasound power. A schematic representation of the experimental set-up for ultrasonic hyperthermia is shown in Fig. 2. The temperature of the sample was monitored using thermometer with two thermocouple sensors T_1 and T_2, which were placed in the center of the ultrasonic beam—1/3rd and 2/3rd the height of the sample from the ultrasonic head, respectively. The measuring system allowed a continuous recording of the temperature inside the sample upon its heating by the ultrasound. Also, a visual IR thermometer that combines surface temperature measurement and real-time thermal and visual images was used.

Fig. 3 presents thermal images of the agar gel phantom before and during ultrasound irradiation. Evidently, the sample is heated under the influence of ultrasound. The temperature of the phantoms increases because of the operation of ultrasound waves generated by the transducer.

Fig. 4 presents temperature measurements in pure agar gels and agar gels with magnetic nanoparticles with concentration of 8 mg/ml and 16 mg/ml, respectively. The figure shows the dependence of the temperature in the phantom on the duration of the ultrasound treatment. The temperature profile of agar gel with sonosensitizers (SPIONs) showed

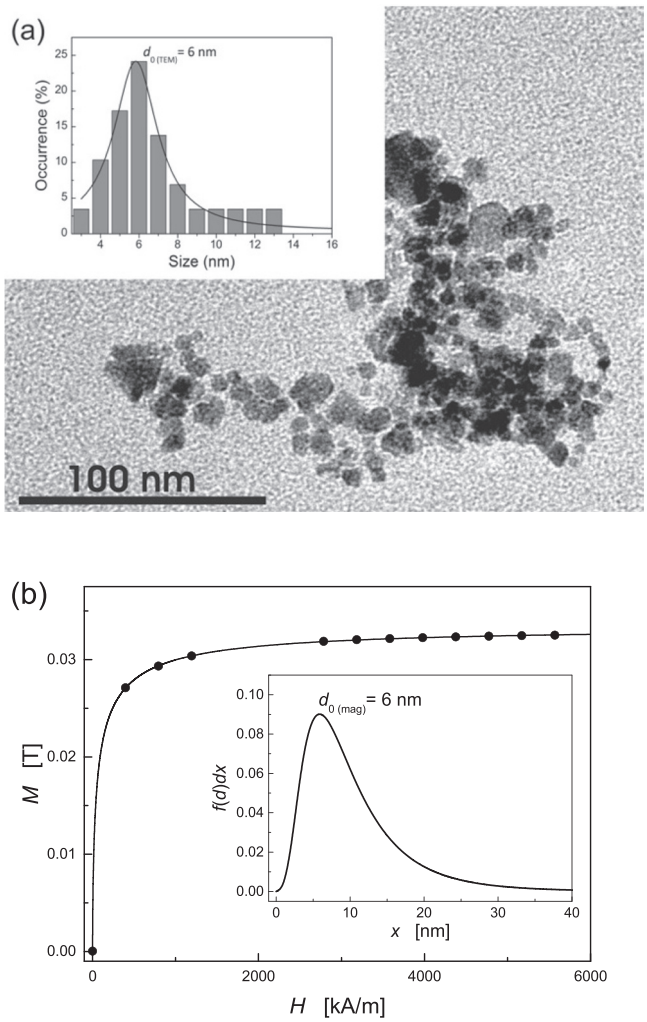

FIG. 1. (a) TEM images with the magnetic particle size distribution and (b) magnetization curve $M(H)$ for the ferrofluid obtained from SQUID data and particle magnetic core size distributions.

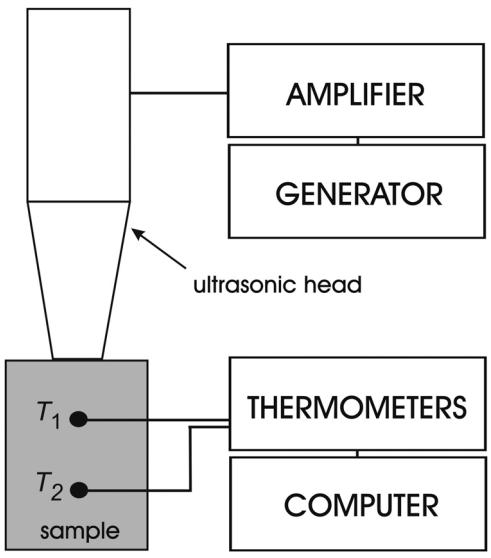

FIG. 2. A block diagram of the experimental set-up for ultrasonic hyperthermia.

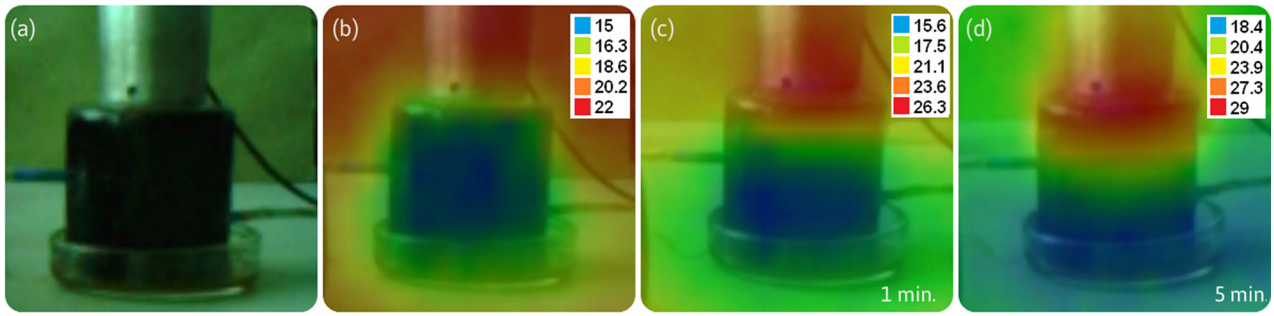

FIG. 3. Pyrometer images of agar gel with magnetic nanoparticles before (a), (b) and during (c), (d) hyperthermia. The images in panels (b)–(d) were obtained by blending visible images with the respective infrared heat maps.

higher heating rates dT/dt in comparison with pure agar gel. In the sample without sonosensitizers, within 5 min the temperature increased by 6 °C, whereas for the samples with the low and high concentration of sonosensitizers, the temperature increased by 10 °C and 15.3 °C, respectively. Thus, an increase of the number of nanoparticles (within the studied range) leads to a better heating effect.

The ultrasound heat generation is the consequence of acoustic wave attenuation. Fig. 5(a) shows the dependence of temperature rise in the phantoms, with and without nanoparticles, on weight percentages of agar. In both samples, a monotonic rise of temperature with the increasing agar concentration can be seen. The increase in ultrasonic attenuation in pure agar gel samples can be explained by the process associated with interactions in the junction zones or aggregates. These interactions are apparently dominated by entropy and volume changes.[18] On the other hand, nanoparticles induce some additional attenuation for acoustic waves that is characteristic for particulate media. It depends in part on the contrast between the physical properties of both the suspended particles and the continuous phase and also on the concentration of solid particles, wavelengths of compression waves, and, in certain cases, thermal wave resulting in heat flow between the material phases.[19] The heating achieved through the sonosensitizing properties of nanoparticles has been observed and explained by the enhanced US attenuation in the region near the nanoparticles. Apparently, the local temperature near each nanoparticle can be significantly higher than the mean one. Attenuation of ultrasonic wave (measured by the pulse-echo technique, $f = 5$ MHz) in samples with 7% concentration of agar is $\alpha = 0.92$ dB/cm without nanoparticles and $\alpha = 1.46$ dB/cm after the addition of sonosensitizers. Fig. 5(b) shows the difference in temperatures measured by sensors placed at two heights on the sample for various concentrations of agar. A decrease in ultrasonic wave intensity and thermal conductivity are responsible for the lower temperature rise at the sample position further away from ultrasonic transducer tip. For the 5% agar-gel sample, after 5 min of US radiation,

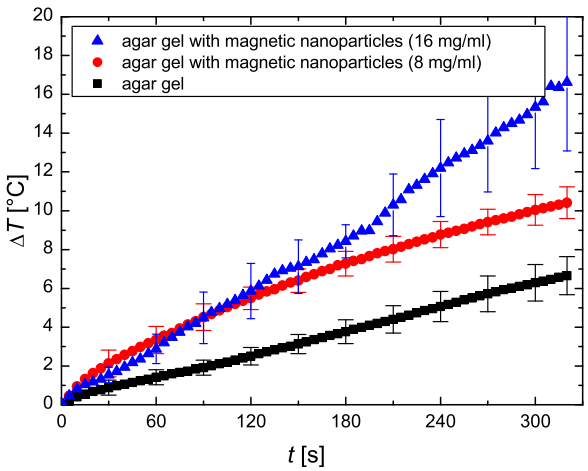

FIG. 4. Hyperthermia curve obtained for agar gel (black squares) and agar gel with magnetic nanoparticles with concentration of 8 mg/ml (red circles) and 16 mg/ml (blue triangles). In both samples, the concentration of agar was 7%.

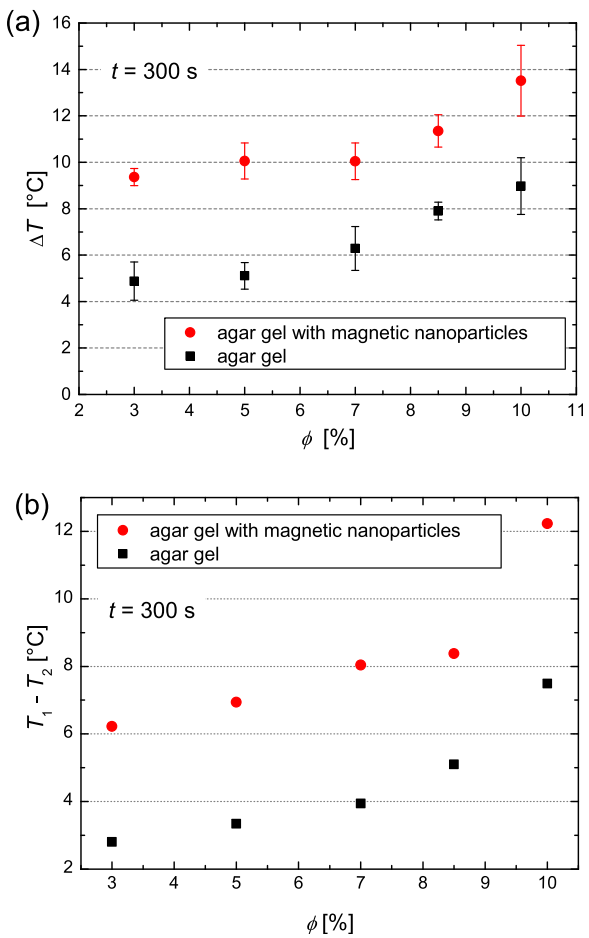

FIG. 5. (a) Temperature change after 5 min of hyperthermia for different concentrations of pure agar gel samples (black squares) and agar gel samples with magnetic nanoparticles (red circles), and (b) the difference in temperatures measured by sensors placed at two heights on the sample.

the first and second thermocouple registered changes of temperatures are, respectively, $\Delta T_1 = 5.1$ °C and $\Delta T_2 = 1.8$ °C for pure agar gel sample and $\Delta T_1 = 10$ °C and $\Delta T_2 = 3.1$ °C for the sample with nanoparticles.

Superparamagnetic iron oxide *particles* can also be used as therapeutic agents for magnetic-field-induced hyperthermia. Magnetic nanoparticles by themselves are able to produce localized heating of the sample when exposed to the alternating magnetic field. The heating effect of magnetic particles is a result of an absorbing energy from the alternating magnetic field and its conversion into heat. There are three mechanisms responsible for this effect: eddy current losses, hysteresis losses during reversal of magnetization, and relaxation losses accompanying demagnetization. In the range of superparamagnetism, the major heating mechanism of nanoparticles is relaxation. Such mechanism has two variants. Néel's relaxation is the flipping of the magnetic moment within a particle by overcoming the magnetic anisotropy energy barrier, $E = KV$ (K – anisotropy constant, V – volume of nanoparticle), without the physical movement of the whole particle. The Brown relaxation mechanism works in a slightly different manner: it causes the rotation of the whole particle in a viscous carrier fluid. These two mechanisms work in parallel. The effective relaxation time, τ, is then dominated by the faster relaxation mechanism.

The effect of magnetic hyperthermia on tissue-mimicking phantoms was determined through calorimetric measurements carried out in the experimental setup described earlier.[20] Temperature was recorded every second using thermometer equipped with an optical fiber sensor (within a thermocouple temperature sensor, the AC magnetic fields can affect thermometer readings by generating eddy currents, which leads to increased temperature in the thermometer itself and its surroundings[20]). Fig. 6 presents examples of temperature change in agar gel and agar gel with magnetite nanoparticle samples under the influence of AMF. The heating effect can be observed in agar gel phantom with magnetite nanoparticles. The rate of the temperature growth was $dT/dt = 3.21$ mK/s. This rather small value of heating rate is probably the result of quenching of Brown relaxation mechanism due to the fixed position of nanoparticles in agar medium. However, this can be compensated by using bigger particles with size range between superparamagnetism and magnetic multi-domains (i.e., 10–100 nm) and utilizing the hysteresis loss mechanism, which shows remarkable dependence on mean size and distribution width.[21] The use of bigger nanoparticles would also increase the efficiency of ultrasonic hyperthermia. The AMF did not influence the temperature in the sample without nanoparticles.

These experiments have shown that magnetic nanoparticles can be used as sonosensitizers for the US-induced hyperthermia and as therapeutic agents for magnetic-field-induced hyperthermia. Magnetic nanoparticles that have been inserted into a tissue not only enhance the effectiveness of ultrasonic hyperthermia because of the increased coefficient of ultrasound absorption but also become the source of additional heating, the amount of which can be controlled by the magnetic field. Our preliminary results shown in Fig. 7 clearly indicate that in the samples with magnetic nanoparticles, the synergetic action of ultrasounds and magnetic field allowed achieving better heating effect in comparison to the heating by either US or AMF alone. This synergistic effect is confirmed by specific absorption rate (SAR) values, which describe overall heating properties of any material. The SAR values were calculated from the formula $SAR = c_p\left(\frac{dT}{dt}\right)_{t=0}$, where c_P is the specific heat capacity of the sample and $(dT/dt)_{t=0}$ is the measured initial slope of the heating curve. The SAR values are 66 mW/g for magnetic hyperthermia, 175 mW/g for ultrasonic hyperthermia, and 375 mW/g for both methods applied simultaneously.

This synergetic application of ultrasonic and magnetic hyperthermia can lead to a promising treatment modality with shorter time regimes, lower intensities of ultrasound, and minimal use of magnetic material delivered to the body. This therapy would be safer for healthy tissues because of better controlled temperature by means of the alternating magnetic field.

In summary, the obtained experimental results demonstrate that magnetic nanoparticles are promising sonosensitizers for ultrasound-induced hyperthermia. The presence of magnetite nanoparticles in the tissue-mimicking phantom increases the absorption of ultrasound energy by the sample,

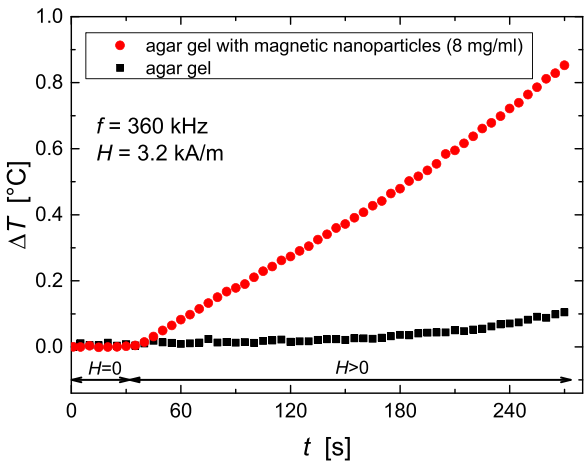

FIG. 6. The recorded temperature change under the influence of the AMF for pure agar gel (black squares) and agar gel with magnetic nanoparticles (red circles). In both samples, the concentration of agar was 7%.

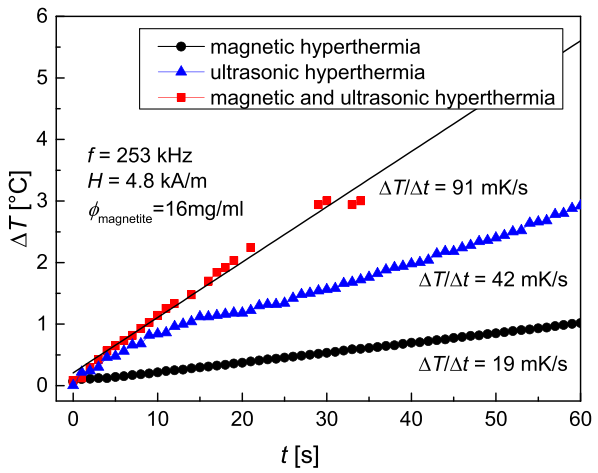

FIG. 7. Temperature change achieved through the synergetic application of ultrasonic and magnetic hyperthermia.

leading to increased temperature. This allows us to use lower doses of ultrasound, that is, with a lower intensity and shorter duration of the US treatment, and still achieve the therapeutic goal. Magnetic nanoparticles can also be used for magnetic hyperthermia—they produce heating of the sample when exposed to the alternating magnetic field. Thus, magnetic hyperthermia and ultrasonic hyperthermia may work synergistically, rather than independently, to produce a more efficient (faster and better controlled reaching of the therapeutic temperature) and safer (lower intensities of US wave and less magnetic material) treatment with minimum side effects.

This work was supported by Grant No. DEC-2015/17/B/ST7/03566 of the Polish National Science Centre and by the Ministry of Education and Science of the Slovak Republic through Grant No. VEGA No. 2/0141/16.

[1]S. Dutz and R. Hergt, Nanotechnology **25**(45), 452001 (2014).
[2]D. Su, R. Ma, M. Salloum, and L. Zhu, Med. Biol. Eng. Comput. **48**(9), 853–863 (2010).
[3]N. P. K. Ellens and K. Hynynen, in *Power Ultrasonics*, edited by K. F. Graff (Woodhead Publishing, Oxford, 2015), pp. 661–693.
[4]J. W. Runt, in *Physics and Technology of Hyperthermia*, edited by S. B. Field and C. Franconi (Martinus Nijhoff Publishers, Dordrecht, Boston, Lancaster, 1987), pp. 354–402.
[5]A. P. Sviridov, L. A. Osminkina, A. L. Nikolaev, A. A. Kudryavtsev, A. N. Vasiliev, and V. Y. Timoshenko, Appl. Phys. Lett. **107**(12), 123107 (2015).
[6]A. Vera, L. Leija, and R. Muñoz, in *Piezoelectric Transducers and Applications*, edited by A. A. Vives (Springer-Verlag, Berlin, Heidelberg, 2008), pp. 467–495.
[7]A. P. Sviridov, V. G. Andreev, E. M. Ivanova, L. A. Osminkina, K. P. Tamarov, and V. Y. Timoshenko, Appl. Phys. Lett. **103**(19), 193110 (2013).
[8]J. Beik, Z. Abed, A. Shakeri-Zadeh, M. Nourbakhsh, and M. B. Shiran, Phys. E **81**, 308–314 (2016).
[9]T. K. Jain, J. Richey, M. Strand, D. L. Leslie-Pelecky, C. A. Flask, and V. Labhasetwar, Biomaterials **29**(29), 4012–4021 (2008).
[10]A. Skumiel, A. Józefczak, M. Timko, P. Kopčanský, F. Herchl, M. Koneracká, and N. Tomašovičová, Int. J. Thermophys. **28**, 1461–1469 (2007).
[11]J. Carrey, V. Connord, and M. Respaud, Appl. Phys. Lett. **102**(23), 232404 (2013).
[12]G. V. Podaru, V. Chikan, and P. Prakash, J. Phys. Chem. C **120**(4), 2386–2391 (2016).
[13]G. Hu and B. He, Appl. Phys. Lett. **100**(1), 013704 (2012).
[14]Y. Gao, C. U. Chan, Q. Gu, X. Lin, W. Zhang, D. C. L. Yeo, A. M. Alsema, M. Arora, M. S. K. Chong, P. Shi, C.-D. Ohl, and C. Xu, NPG Asia Mater. **8**, e260 (2016).
[15]M. Koneracká, P. Kopčanský, M. Timko, and C. N. Ramchand, J. Magn. Magn. Matter. **252**, 409–411 (2002).
[16]T. D. Mast, Acoust. Res. Lett. Online **1**(2), 37–42 (2000).
[17]A. Skumiel, A. Józefczak, K. Hellller, T. Hornowski, and K. Wielgusz, Arch. Acoust. **38**(3), 297–301 (2013).
[18]W. J. Gettins, P. L. Jobling, and E. Wyn-Jones, J. Chem. Soc., Faraday Trans. 2 **74**, 1246–1252 (1978).
[19]R. E. Challis, M. J. W. Povey, M. L. Mather, and A. K. Holmes, Rep. Prog. Phys. **68**, 1541–1637 (2005).
[20]A. Skumiel, T. Hornowski, A. Józefczak, M. Koralewski, and B. Leszczyński, Appl. Therm. Eng. **100**, 1308–1318 (2016).
[21]R. Hergt, S. Dutz, and M. Röder, J. Phys.: Condens. Matter **20**(38), 385214 (2008).